

YALE PEABODY MUSEUM

P.O. BOX 208118 | NEW HAVEN CT 06520-8118 USA | PEABODY.YALE. EDU

JOURNAL OF MARINE RESEARCH

The *Journal of Marine Research*, one of the oldest journals in American marine science, published important peer-reviewed original research on a broad array of topics in physical, biological, and chemical oceanography vital to the academic oceanographic community in the long and rich tradition of the Sears Foundation for Marine Research at Yale University.

An archive of all issues from 1937 to 2021 (Volume 1–79) are available through EliScholar, a digital platform for scholarly publishing provided by Yale University Library at <https://elischolar.library.yale.edu/>.

Requests for permission to clear rights for use of this content should be directed to the authors, their estates, or other representatives. The *Journal of Marine Research* has no contact information beyond the affiliations listed in the published articles. We ask that you provide attribution to the *Journal of Marine Research*.

Yale University provides access to these materials for educational and research purposes only. Copyright or other proprietary rights to content contained in this document may be held by individuals or entities other than, or in addition to, Yale University. You are solely responsible for determining the ownership of the copyright, and for obtaining permission for your intended use. Yale University makes no warranty that your distribution, reproduction, or other use of these materials will not infringe the rights of third parties.



This work is licensed under a Creative Commons Attribution-NonCommercial-ShareAlike 4.0 International License.
<https://creativecommons.org/licenses/by-nc-sa/4.0/>



*Free Oscillations in a Beta-plane Ocean*¹

H. O. Mofjeld² and Maurice Rattray, Jr.

*Department of Oceanography
University of Washington
Seattle, Washington 98105*

ABSTRACT

This paper is concerned with the free oscillations in a rectangular equatorial beta-plane model of large oceans with a free surface placed symmetrically on the equator. With the depth constant and the stratification horizontally uniform, the motion may be separated into vertical modes, each having free oscillations. The primary emphasis is on the surface oscillations, which are of two distinct types: the gravity oscillations with periods of 1.6 days or less and the Rossby oscillations with periods of several days or greater. These periods turn out to be strong functions of the ocean's shape and nondimensional size. The gravity oscillations are either dynamically similar to Kelvin waves or Poincaré waves; the latter is the only kind of oscillation restricted to latitudes below the critical latitude. The Rossby oscillations consist primarily of Rossby waves that propagate under modulating envelopes that produce some equatorial trapping.

Introduction. We are concerned here with the free oscillations in a rectangular beta-plane ocean with a free surface. The equator is parallel to the zonal coasts and bisects the ocean into symmetrical northern and southern halves. The ocean possesses several features that have an important effect on the time-dependent dynamics of the real oceans; it has boundaries in longitude as well as latitude, the Coriolis parameter varies significantly over the ocean, and the motion is subject simultaneously to gravity and a varying Coriolis parameter. We take the total depth to be constant and the density to be a function only of the vertical coordinate; this allows the motion to be uncoupled into vertical modes. The primary emphasis here is on free oscillations in the surface mode.

In this ocean there are two types of oscillations that are analogous to the oscillations of the first and second classes in an unbounded spherical ocean. The high-frequency or gravity oscillations show considerable similarity to the oscillations in rectangular oceans with a constant Coriolis parameter. The latter

1. Contribution 598 from the Department of Oceanography, University of Washington. This investigation was supported by the National Science Foundation under Grant GA-22692.

Accepted for publication and submitted to press 15 June 1971.

2. Present address: Atlantic Oceanographic and Meteorological Laboratories, NOAA, Miami, Florida 33130.

have been studied by many authors, among them Rao (1966), who has given the most exhaustive treatment both theoretically and experimentally in the laboratory.

Rattray and Charnell (1966) found approximate forms of the low-frequency or Rossby oscillations, which consist of pairs of separable solutions to the dynamic equations. We will see that these quasigeostrophic oscillations do resemble the Rossby oscillations in the surface mode.

Using the same beta-plane ocean, Moore (1968) considered the internal oscillations; but, since a basic assumption of his analysis is that the motion near the high-latitude coasts is well separated from the equatorial region, it cannot be used to obtain the surface oscillations. Like Moore, we also will write the free oscillations as sums of the separable solutions to the dynamic equations. Instead of dividing the ocean into separate regions, between which Moore matched the amplitudes and phases of the motion, we will transform the boundary conditions at the eastern and western coasts into a matrix equation that determines the frequencies and amplitudes of the separable solutions. In doing so we are following the procedure that was introduced by Taylor (1922) in his treatment of free oscillations in rectangular oceans with a constant Coriolis parameter.

Longuet-Higgins (1968) has discussed the connection between the free oscillations on the unbounded spherical ocean and those on the corresponding equatorial beta plane. Longuet-Higgins and Pond (1970) also compared Moore's results with internal oscillations in a spherical ocean bounded by two meridians 180° apart.

Analysis. The ocean considered is illustrated in Fig. 1; it lies on an equatorial beta plane between $y = \pm y_0$, with the equator at $y = 0$. It is convenient to place the origin of the rectangular coordinate system midway between the meridional coasts, which then lie at $x = \pm x_0$. We take the total depth, h , to be constant and require that the side boundaries be vertical. The unperturbed density, ρ_0 , depends only on the vertical coordinate, z , which is positive upward. The acceleration of gravity, g , is constant, and the Coriolis parameter is given by $f = \beta y$. We let the velocity components (u, v, w) correspond to (x, y, z) , respectively, and let P be the pressure and ρ the density.

Assuming that x and y are positive eastward and northward, respectively, and that t represents time, the linearized equations of motion are written

$$u_t - \beta y v = -\frac{1}{\rho_0} P_x, \quad (1)$$

$$v_t + \beta y u = -\frac{1}{\rho_0} P_y, \quad (2)$$

and, making the hydrostatic approximation,

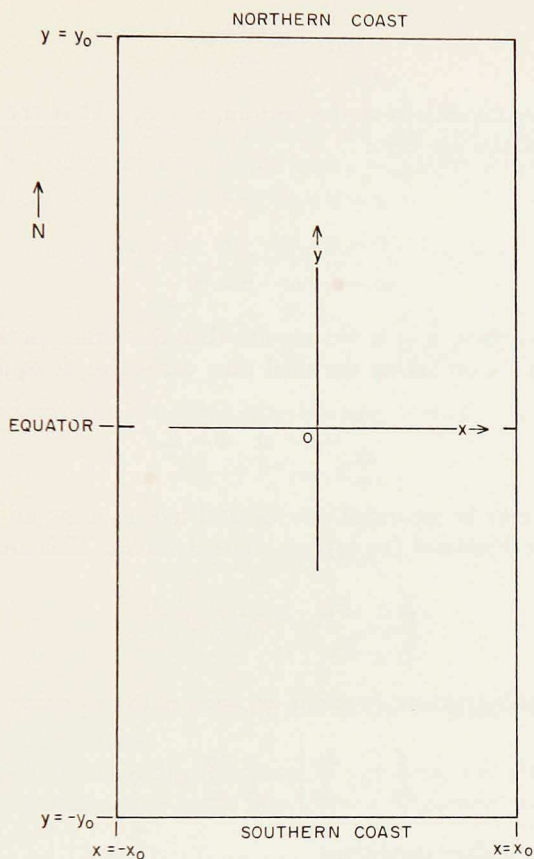


Figure 1. Rectangular ocean placed symmetrically on the equator of an equatorial beta plane. The origin of the rectangular coordinate system is at the center of the ocean, with x positive eastward and y positive northward.

$$\circ = -P_z - \rho g, \quad (3)$$

where the subscripts denote partial differentiation.

Taking the water to be incompressible, the equation of continuity is

$$u_x + v_y + w_z = \circ; \quad (4)$$

defining a density perturbation, ρ_1 , by

$$\rho = \rho_0 + \rho_1, \quad (5)$$

the linearized equation expressing incompressibility is then

$$(\rho_1)_t + w \frac{d\rho_0}{dz} = 0. \quad (6)$$

The boundary conditions at the bottom, $z = 0$, and at the coasts are that the normal velocities are zero:

$$u = 0 \quad \text{at} \quad x = \pm x_0, \quad (7)$$

$$v = 0 \quad \text{at} \quad y = \pm y_0, \quad (8)$$

and

$$w = 0 \quad \text{at} \quad z = 0. \quad (9)$$

At the free surface, $z = h$, we require that the atmospheric pressure, P_0 , be constant, which, on taking the total time derivative, is equivalent to

$$\frac{dP}{dt} = 0 \quad \text{at} \quad z = h. \quad (10)$$

The motion may be separated into vertical modes, using an analysis similar to that given by Fjeldstad (1933) for internal waves. This analysis (Mofjeld 1970) yields

$$\left(u, v, \frac{P_1}{\rho_0} \right) = (U, V, gZ) \frac{d\psi}{dz}, \quad (11)$$

where the vertical-structure function, ψ , satisfies the equation

$$\frac{d}{dz} \left[\rho_0 \frac{d\psi}{dz} \right] - \frac{1}{H} \frac{d\rho_0}{dz} \psi = 0 \quad (12)$$

subject to the boundary conditions

$$\psi = 0 \quad \text{at} \quad z = 0 \quad (13)$$

and

$$\frac{d\psi}{dz} - \frac{1}{H} \psi = 0 \quad \text{at} \quad z = h; \quad (14)$$

H is the eigenvalue.

For the zero vertical surface mode, H is very close to the actual depth, h , and ψ is nearly linear in z . The amplitudes U and V are then essentially the horizontal velocities, and Z is the surface elevation.

For a given mode, eqs. (1), (2), and (4) become

$$U_t - \beta y V = -gZ_x, \quad (15)$$

$$V_t + \beta y U = -gZ_y, \quad (16)$$

$$Z_t + H(U_x + V_y) = 0, \quad (17)$$

and at the coasts we have

$$U = 0 \quad \text{at} \quad x = \pm x_0 \quad (18)$$

and

$$V = 0 \quad \text{at} \quad y = \pm y_0. \quad (19)$$

To nondimensionalize these equations, we use scale factors commonly employed for the equatorial beta plane; with $c = (gH)^{1/2}$ written for the phase velocity of a long gravity wave, we take

$$x' = (\beta/c)^{1/2} x, \quad y' = (\beta/c)^{1/2} y, \quad t' = (\beta c)^{1/2} t \quad (20)$$

and

$$U' = \frac{U}{U_0}, \quad V' = \frac{V}{U_0}, \quad Z' = \frac{c}{H} \frac{Z}{U_0}. \quad (21)$$

The nondimensional equations then have the same form for each vertical mode:

$$U'_{t'} - y' V' = -Z'_{x'}, \quad (22)$$

$$V'_{t'} + y' U' = -Z'_{y'}, \quad (23)$$

$$Z'_{t'} + U'_{x'} + V'_{y'} = 0, \quad (24)$$

$$U' = 0 \quad \text{at} \quad x' = \pm x'_0, \quad (25)$$

and

$$V' = 0 \quad \text{at} \quad y' = \pm y'_0. \quad (26)$$

The difference between vertical modes lies in the nondimensional size of the ocean and in the time scale.

SEPARABLE SOLUTIONS. By separation of variables, we obtain solutions to (22) through (24) that satisfy (26); they consist of Kelvin waves,

$$\begin{Bmatrix} U_0^{(\pm)} \\ V_0^{(\pm)} \\ Z_0^{(\pm)} \end{Bmatrix} = \begin{Bmatrix} 1 \\ 0 \\ \pm 1 \end{Bmatrix} e^{\pm y'^2/2} e^{i(\sigma' t' \pm \sigma' x)}, \quad (27)$$

and gravity-Rossby waves,

$$\begin{Bmatrix} U_n^{(\pm)} \\ V_n^{(\pm)} \\ Z_n^{(\pm)} \end{Bmatrix} = e^{i(\sigma' t' + [(1/2)\sigma' \pm R_n] x')} \begin{Bmatrix} \sigma' y' Y_n + [(1/2)\sigma'] \pm R_n \frac{dY_n}{dy'} \\ -i\{[(1/2)\sigma'] \pm R_n\}^2 - \sigma' \alpha'^2 \} Y_n \\ -[(1/2)\sigma'] \pm R_n y' Y_n - \sigma' \frac{dY_n}{dy'} \end{Bmatrix}, \quad (28)$$

where the Weber function, $Y_n(y')$, satisfies

$$\frac{d^2 Y_n}{dy'^2} + (\alpha_n - y'^2) Y_n = 0, \quad (29)$$

$$\text{with} \quad Y_n = 0 \quad \text{at} \quad y' = \pm y'_0, \quad (30)$$

$$\text{and where} \quad R_n = \left[\sigma'^2 + \frac{1}{4\sigma'^2} - \alpha_n \right]^{1/2}. \quad (31)$$

For a given n , there is a range of frequency, σ' , over which R_n is imaginary; conversely, for a given σ' , R_n is imaginary for all n greater than some n_0 . In either case we take

$$S_n = -iR_n; \quad (32)$$

the corresponding gravity-Rossby waves are bound to one of the two meridional coasts, $x' = \pm x'_0$.

MATRIX EQUATION. To satisfy the remaining boundary conditions (25), we write each free oscillation as a sum of Kelvin and gravity-Rossby waves

$$\begin{Bmatrix} U \\ V \\ Z \end{Bmatrix} = \sum_{n=0}^{\infty} \begin{Bmatrix} a_n U_n^{(+)} + b_n U_n^{(-)} \\ a_n V_n^{(+)} + b_n V_n^{(-)} \\ a_n Z_n^{(+)} + b_n Z_n^{(-)} \end{Bmatrix}. \quad (33)$$

At $x' = \pm x'_0$ we then have

$$\left. \begin{aligned} & a_0 e^{\pm i\sigma' x'_0} \gamma_0 + b_0 e^{\mp i\sigma' x'_0} \delta_0 \\ & + \sum_{n=1}^{n_0} [a_n e^{\pm [(1/2)\sigma'] + R_n} x'_0 \gamma_n + b_n e^{\pm [(1/2)\sigma'] - R_n} x'_0 \delta_n] \\ & + \sum_{n=n_0+1}^{\infty} [a_n e^{\pm [(1/2)\sigma'] - S_n} x'_0 (\lambda_n + i\mu_n) + b_n e^{\pm [(1/2)\sigma'] + S_n} x'_0 (\lambda_n - i\mu_n)] = 0, \end{aligned} \right\} \begin{array}{l} (34a) \\ (34b) \end{array}$$

where

$$\left. \begin{aligned} \left\{ \begin{array}{l} \gamma_0 \\ \delta_0 \end{array} \right\} &= e^{\pm y'^2/2}, \quad \left\{ \begin{array}{l} \gamma_n \\ \delta_n \end{array} \right\} = \sigma' y' Y_n + [(1/2)\sigma'] \pm R_n \frac{dY_n}{dy'}, \\ \lambda_n &= \sigma' y' Y_n + \frac{1}{2\sigma'} \frac{dY_n}{dy'}, \quad \mu_n = S_n \frac{dY_n}{dy'}. \end{aligned} \right\} \quad (35)$$

If we take the complex conjugate of (34b), the terms that multiply the amplitudes for a given n are identical to those in (34a); for these equations to be consistent, the amplitudes must satisfy the conditions

$$\left. \begin{aligned} a_n^* &= Ba_n, & b_n^* &= Bb_n, & 0 \leq n \leq n_0, \\ b_n^* &= Ba_n, & a_n^* &= Bb_n, & n_0 < n, \end{aligned} \right\} \quad (36)$$

where the asterisk denotes the complex conjugate and B is a complex constant.

The conditions for $n_0 < n$ require that B have unit modulus

$$B = e^{2i\varphi}.$$

By adjusting the initial time, $e^{i\sigma' t'} \rightarrow e^{i(\sigma' t' - \varphi)}$, we obtain the following conditions on the amplitudes:

$$a_n, b_n \text{ are real, } 0 \leq n \leq n_0,$$

$$\begin{cases} a_n \\ b_n \end{cases} = c_n \pm id_n, \quad n_0 < n, \quad (38)$$

where c_n and d_n are real.

To find the frequencies of the free oscillations and the amplitudes of the separable solutions, we expand the boundary condition (34a) in a series of Weber functions, $\Phi_m(\gamma')$, that satisfy

$$\frac{d^2 \Phi_m}{dy'^2} + (\tau_m - y'^2) \Phi_m = 0, \quad (39)$$

with

$$\frac{d\Phi_m}{dy'} = 0 \quad \text{at} \quad y' = \pm y'_0. \quad (40)$$

By the orthogonality of the basic set $\{\Phi_m\}$, the amplitudes must satisfy the following set of simultaneous linear equations:

$$\left. \begin{aligned} & a_0 e^{i\sigma' x'_0} \gamma_{0,m} + b_0 e^{-i\sigma' x'_0} \delta_{0,m} \\ & + \sum_{n=1}^{n_0} [a_n e^{i[(1/2)\sigma' + R_n] x'_0} \gamma_{n,m} + b_n e^{i[(1/2)\sigma' - R_n] x'_0} \delta_{n,m}] \\ & + \sum_{n=n_0+1}^{\infty} [(c_n + id_n) e^{[(1/2)\sigma' - S_n] x'_0} (\lambda_{n,m} + i\mu_{n,m}) \\ & + (c_n - id_n) e^{[(1/2)\sigma' + S_n] x'_0} (\lambda_{n,m} - i\mu_{n,m})] = 0, \end{aligned} \right\} \quad (41)$$

where $\gamma_{0,m}$, $\delta_{0,m}$, etc., are given in the APPENDIX, p. 303.

After taking the real and imaginary parts of (41), we obtain a set of equations that may be put into matrix form,

$$U\vec{A} = \vec{0}, \quad (42)$$

where U is a matrix whose elements are given in the APPENDIX and \vec{A} is the amplitude vector. In practice it is convenient to separate (42) into two matrix equations, one corresponding to oscillations for which Z is symmetrical about the equator and the other for which Z is antisymmetrical.

A sequence of computer programs was used to calculate the frequencies of oscillation and the distributions of the dynamic variables (U, V, Z). The eigenvalues of the Weber functions were computed from a matrix equation derived by expanding the Weber function in a Fourier series and by substituting the

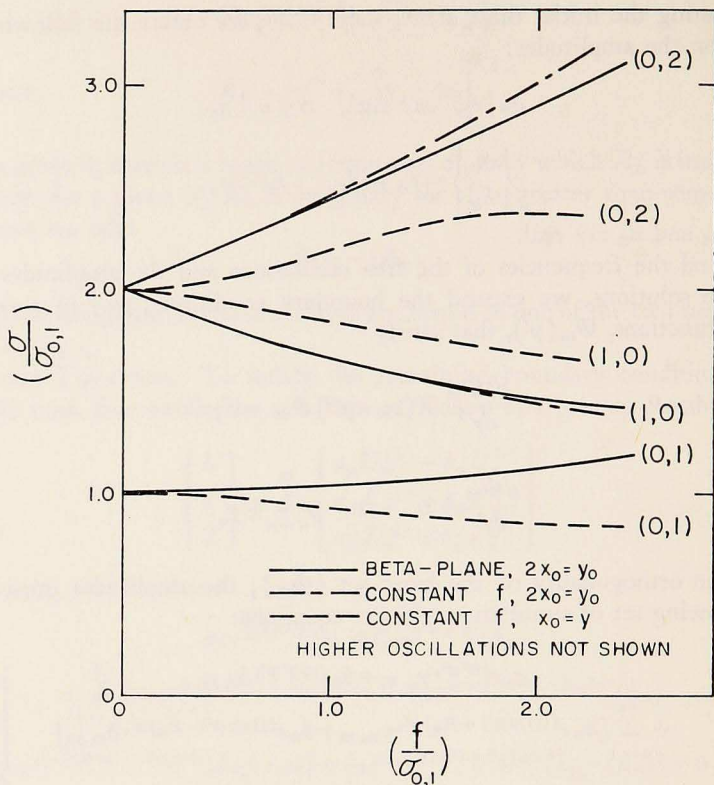


Figure 2a. Frequencies of oscillation: Gravity oscillations for the beta-plane ocean, with $2x_0 = y_0$ and oscillations for constant f (from Rao 1966).

series into the ordinary differential equation. The Weber functions were then found by integrating the differential equation, using Milne's method (Scarborough 1966).

For given values of x'_0 and y'_0 , the frequency was then scanned until a zero was found in the determinant of U , which is the requirement that the amplitudes be nonzero. When the amplitudes had been computed, the series (36) were then summed to give the dynamic variables. The calculations were done mainly on IBM 7094 and CDC 6400 computers at the University of Washington, with contouring and other subsidiary work done on an IBM 1130.

How well the series in U converged to the boundary conditions at $x' = \pm x'_0$ is one measure of the accuracy of these calculations. For surface oscillations with the matrix truncated at $n = 10$, the value of U along these coasts was a few tenths of a per cent of the maximum velocity in the interior, except for the corners ($\pm x_0, \pm y_0$), where it was less than 5%. On using a large matrix, with the order increased to include $n = 15$, it was found that the frequencies

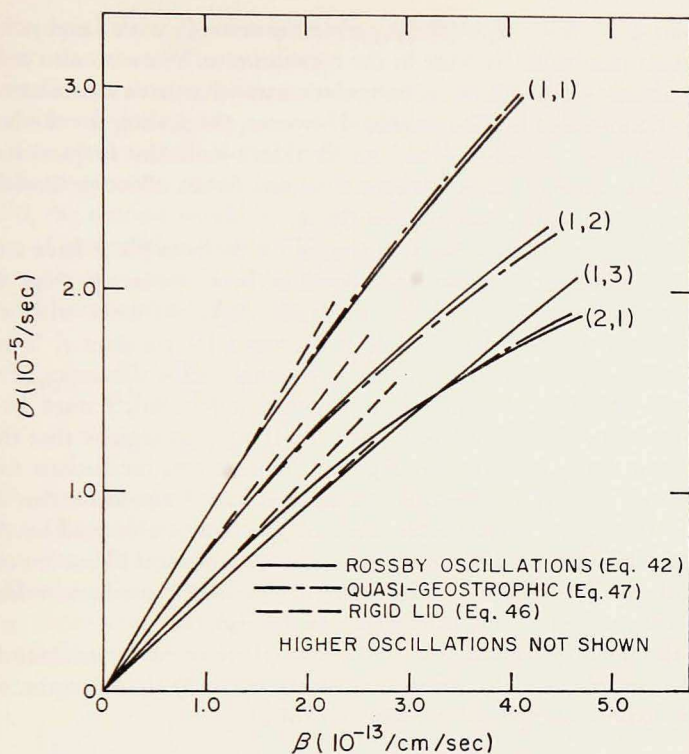


Figure 2b. Frequencies of oscillation: Rossby oscillations for the beta-plane ocean, with $2x_0 = y_0$ and rigid-lid (gravity effects suppressed) and approximate quasigeostrophic oscillations; $\beta = 2.3(10)^{-13} \text{ cm}^{-1} \text{ sec}^{-1}$, $H = 4000 \text{ m}$.

were essentially unchanged; and, while the boundary conditions were better satisfied, the motion in the interior was not significantly affected.

Frequencies of Oscillation. GRAVITY OSCILLATIONS. We begin the description of the free oscillations by considering their frequencies. One set of oscillations becomes the free oscillations in the nonrotating ocean as the rotation rate is reduced to zero; they are therefore analogous to class 1 oscillations in an unbounded ocean on a spherical earth. The other set, which we will discuss later, is analogous to class 2 oscillations.

Without rotation, the frequencies of oscillations in a rectangular ocean are given by

$$\sigma_{m,n} = \pi c \left[\left(\frac{m}{2x_0} \right)^2 + \left(\frac{n}{2y_0} \right)^2 \right]^{1/2}; \quad m, n = 0, 1, \dots \quad (43)$$

To show how the gravity oscillations depend on the rotation rate, we have chosen a rectangular ocean with $2x_0 = y_0$ and have computed the frequencies

as functions of y'_0 . Since $y'_0 = (\beta/c)y_0$, an increase in y'_0 , with c and y_0 held constant, is equivalent to an increase in the rotation rate. We wish also to compare these frequencies with those in rectangular oceans that have a constant Coriolis parameter f , computed by Rao (1966). However, the scaling for the beta plane is inappropriate for constant f , and we therefore scale the frequencies on the fundamental frequency, $\sigma_{0,1}$, without rotation. As an effective Coriolis parameter on the beta plane, we take $\bar{f} = \beta y_0/2$.

We see from Fig. 2a that the frequencies on the beta plane have a different dependence on the rotation rate than do those in a constant f ocean with the same shape. The frequency of the oscillation (0,1) increases with a greater rotation rate on the beta plane while it decreases for constant f . The reason for the discrepancy is that the equator is essential to the dynamics of the beta plane ocean. To have an equator on a constant f ocean, f must be zero; a comparison with $f \neq 0$ is therefore not valid if we also require that the ocean have the same shape and size. In Fig. 2a, the next two oscillations for which the meridional velocity V is zero at the equator have frequencies that are close to those in the square oceans with constant f , which are formed by placing a boundary at the equator. Evidently, then, the equator acts like a boundary for this type of gravity oscillation. This cannot be true for oscillations like (0,1), whose meridional velocities are nonzero at the equator.

When the nondimensional size of the beta-plane ocean is sufficiently large, the frequencies obtained by using the matrix eq. (42) should agree with the asymptotic expression derived by Moore (1968):

$$\sigma'(2x'_0 + y'_0) - \arcsin \left[\frac{(1/2\sigma') + \sigma'}{(2)^{1/2}} \right] + C(\sigma') = m\pi; \quad m = 1, 2, \dots \quad (44)$$

where

$$C(\sigma') = \lim_{k \rightarrow \infty} \left\{ \sum_{l=1}^k \arcsin \left[\frac{(1/2\sigma') + \sigma'}{(l)^{1/2}} \right] - \left(\frac{1}{2\sigma'} + \sigma' \right) (k)^{1/2} \right. \\ \left. - \sum_{l=1}^k \arcsin \left[\frac{1/(2\sigma') - \sigma'}{2(l+1/2)^{1/2}} \right] + \left(\frac{1}{2\sigma'} - \sigma' \right) (k+1/2)^{1/2} \right\}, \quad (45)$$

which is valid within the frequency range where R_1 is imaginary. Taking $x'_0 = y'_0 = 4.950$, we see from Table I that the frequencies obtained by the two approaches are in good agreement.

To model the surface oscillations in the Atlantic and Pacific oceans, we assume that $\beta = 2.30(10)^{-13} \text{ sec}^{-1} \text{ cm}^{-1}$, $H = 4000 \text{ m}$, and $y_0 = 6.25(10)^3 \text{ km}$, which gives a nondimensional extent in latitude of $y'_0 = 2.12$. In Table IIa the periods in days are given for $0.25y_0 \leq x_0 \leq 1.0y_0$. Since the Atlantic Ocean is narrow, it corresponds to a small value of the aspect ratio, x_0/y_0 , while the Pacific Ocean corresponds to a larger value. We see from Table II that the

periods are equal to, or less than, 1.6 days, and their range includes the periods of the diurnal and semidiurnal tides.

ROSSBY OSCILLATIONS. Let us turn now to the Rossby oscillations, which, since their frequencies go to zero as the rotation rate is reduced to zero, are analogous to class 2 oscillations. If the ocean consisted of homogeneous water and were covered by a rigid lid, the motion would be governed by conservation of potential vorticity. The free oscillations in such an ocean would consist of Rossby waves, with frequencies given by

$$\left. \begin{aligned} \sigma_{m,n} &= \frac{\beta}{2\pi} \left[\left(\frac{m}{2x_0} \right)^2 + \left(\frac{n}{2y_0} \right)^2 \right]^{-1/2}; \\ m, n &= 1, 2, \dots \end{aligned} \right\} \quad (46)$$

With a free surface and stratification, Rattray and Charnell (1966) assumed that the Rossby oscillations could be approximated by pairs of gravity-Rossby waves (28), and they obtained the following expression for the frequencies of these quasigeostrophic oscillations:

$$\left(\frac{\beta}{2\sigma_{m,n}} \right)^2 + \left(\frac{\sigma_{m,n}}{c} \right)^2 - \frac{\beta}{c} \alpha_n = \left(\frac{m\pi}{2x_0} \right)^2; \quad m, n = 1, 2, \dots \quad (47)$$

To show how the frequencies of the Rossby oscillations depend on the rotation rate, we again chose a rectangular ocean, with $2x'_0 = y'_0$, and computed the frequencies as functions of y'_0 , using the matrix eq. (42). In Fig. 2b these frequencies are plotted in dimensional form versus β , with c and y_0 held constant. The divergence of the frequencies obtained from (42) and (47) from the rigid-lid frequencies (46) is due to the combined effect of gravity and beta, which produces equatorial trapping. The agreement between the frequencies from (42) and the quasigeostrophic frequencies (47) indicates that the Rossby oscillations are made up principally of single pairs of gravity-Rossby waves, as Rattray and Charnell had assumed.

In Table IIb, the periods (in days) of Rossby oscillations are given for $y'_0 = 2.12$; these oscillations correspond to the surface oscillations in the Atlantic and Pacific oceans. A range of x_0/y_0 is used to indicate the strong dependence of the periods on this aspect ratio; as with the gravity oscillations, the sequence of the Rossby oscillations is a function of both the size and the shape of the ocean. The periods of the Rossby oscillations are 2.6 days or greater, and, for wider oceans, they include the 4-5-day-period range at which the lower tropical atmosphere fluctuates.

Table I. Comparison of nondimensional frequencies (σ') of oscillation obtained from the matrix equation (45) and the asymptotic expression (47) of Moore (1968).

Matrix equation	Asymptotic expression
0.48	0.47
0.70	0.69
0.93	0.91
1.15	1.13
1.37	1.34
1.57	1.55

$$x'_0 = y'_0 = 4.950.$$

Table II. Periods of the free oscillations, in days, for the surface mode in large oceans with $y_0 = 6.25(10)^3$ km, $\beta = 2.3(10)^{-13}$ cm $^{-1}$ sec $^{-1}$, $H = 4000$ m.

a. GRAVITY OSCILLATIONS

Z antisymmetrical about the equator

(m, n)	$x_0 = 0.25y_0$	$x_0 = 0.50y_0$	$x_0 = 0.75y_0$	$x_0 = 1.00y_0$
(0,1)	1.40	1.36	1.34	1.33
(1,1)	0.51	0.67	0.83	0.94
(0,3)	0.33	0.42	0.44	0.48
(1,3)	0.30	0.42	0.53	0.64

Z symmetrical about the equator

(1,0)	0.74	0.92	1.25	1.60
(0,2)	0.39	0.55	0.68	0.83
(1,2)	0.34	0.53	0.59	0.62
(2,0)	0.30	0.36	0.42	0.55

b. ROSSBY OSCILLATIONS

Z antisymmetrical about the equator

(m, n)	$x_0 = 0.25y_0$	$x_0 = 0.50y_0$	$x_0 = 0.75y_0$	$x_0 = 1.00y_0$
(1,1)	6.70	3.80	3.00	2.60
(2,1)	13.80	6.70	4.80	3.80
(3,1)	19.30	9.80	6.70	5.20
(1,3)	8.40	6.20	5.80	5.60

Z symmetrical about the equator

(1,2)	7.40	4.90	4.40	4.20
(2,2)	13.20	7.60	5.70	5.00
(3,2)	19.50	10.40	7.40	6.10
(1,4)	9.30	7.40	7.20	7.00

Coupling between Oscillations. Longuet-Higgins and Pond (1970) found that no two oscillations in a rotating hemispherical ocean, with the poles on the boundary, could have the same frequency. As the rotation rate changes, two oscillations whose frequencies are converging become coupled; the curves then do not cross but form the branches of a hyperbola.

To see whether the oscillations in the rectangular beta-plane oceans have such behavior, it is convenient to keep the rotation rate fixed and to vary the aspect ratio, x_0/y_0 . If two oscillations have the same frequencies, we may turn around and approach the degeneracy by fixing x_0/y_0 and by varying the rotation rate. In Fig. 3 we see that the frequency curves do not cross in the beta-plane oceans. Away from the point of closest approach, the oscillations are uncoupled; the oscillation with the lower (upper) curve is similar to that with the upper (lower) curve on the other side of the coupled region. In this sense the oscillations have crossed from one curve to the other; a given oscillation may be labeled by the mode numbers (m, n) at a small rotation rate, provided that it is not strongly coupled to other oscillations.

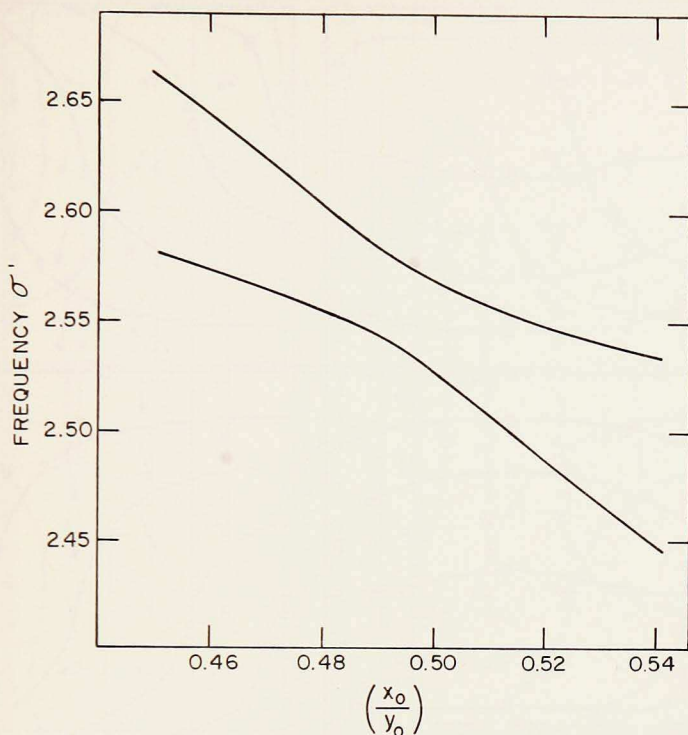


Figure 3. Two approaching frequency curves showing that such curves do not intersect; the oscillation with the lower (upper) curve is similar to that with the upper (lower) curve on the opposite side of the coupled region. This phenomenon was first found by Longuet-Higgins and Pond (1970) for a hemispherical ocean.

To see why coupling occurs, it is convenient to consider the Rossby oscillations, each of which is ordinarily dominated by a single pair of gravity-Rossby waves. The other waves act to satisfy more exactly the boundary conditions at $x' = \pm x'_0$, and ordinarily they have a small amplitude. However, if another pair of gravity-Rossby waves is near resonance, i.e., nearly satisfies these boundary conditions themselves, it must have a large amplitude in the interior to make its contribution to the oscillation adjacent to the boundary. Since they, in general, constitute the major part of another oscillation, we may say that the oscillations have become coupled.

Dynamic Variables. While frequencies give some insight into the free oscillations, it is necessary also to consider the dynamic variables (U, V, Z) to obtain a complete description. In this section we give examples of the free oscillations in an ocean with $2x'_0 = y'_0 = 2.12$, corresponding to the surface mode in the Pacific Ocean.

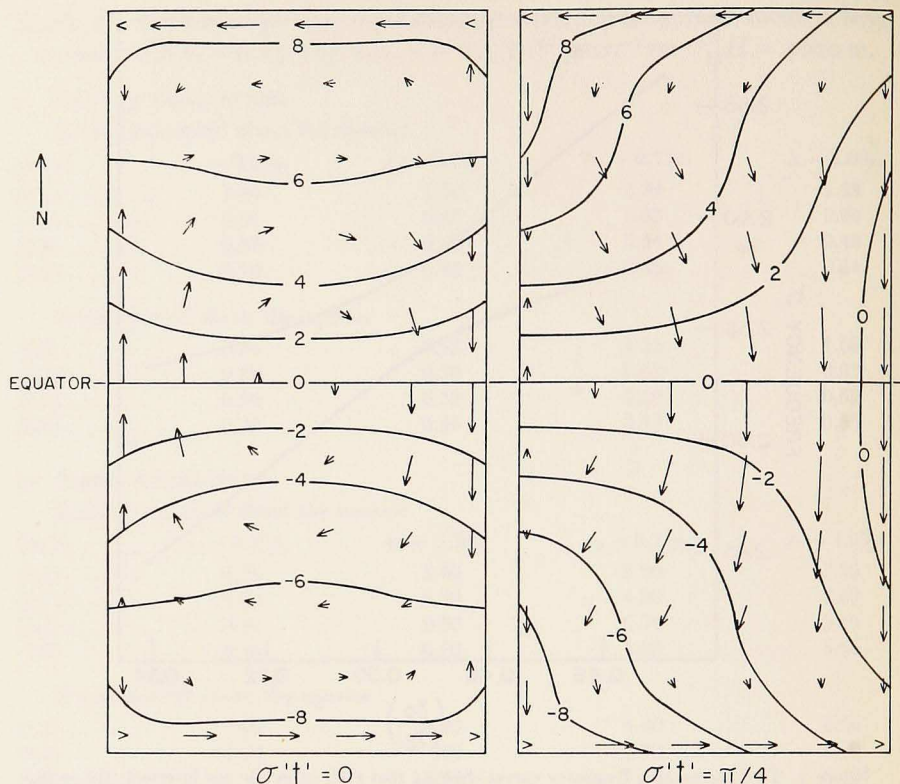


Figure 4a. Gravity oscillation (0,1), with the lowest frequency for $2x'_0 = y'_0 = 2.12$; period = 1.36 days for $\beta = 2.3(10)^{-13} \text{ cm}^{-1} \text{ sec}^{-1}$, $y_0 = 6.25(10)^3 \text{ km}$. The contours are lines of constant surface elevation, and the arrows are horizontal velocities at the tails of the arrows. See also opposite page.

GRAVITY OSCILLATIONS. The gravity oscillation (0,1) is illustrated in Fig. 4, where the contours are lines of constant surface elevation and the arrows are horizontal velocities at the tails of the arrows. Both surface elevation, Z , and zonal velocity, U , are antisymmetric about the equator while the meridional velocity, V , is symmetric. The pattern of surface contours rotates counterclockwise north of the equator and clockwise to the south; in both halves of the ocean the velocity pattern appears to propagate westward. Near the high-latitude coasts, $y' = \pm y'_0$, the velocity tends toward geostrophic balance with the surface slopes, as in a Kelvin wave.

The second gravity oscillation (1, 0), given in Fig. 5, has surface elevations and zonal velocities that are symmetric about the equator while the meridional velocity is antisymmetric. Again the surface contours rotate counterclockwise in the northern half and clockwise in the southern half of the ocean. The velocity tends toward geostrophic balance with Z over the entire ocean. This oscil-

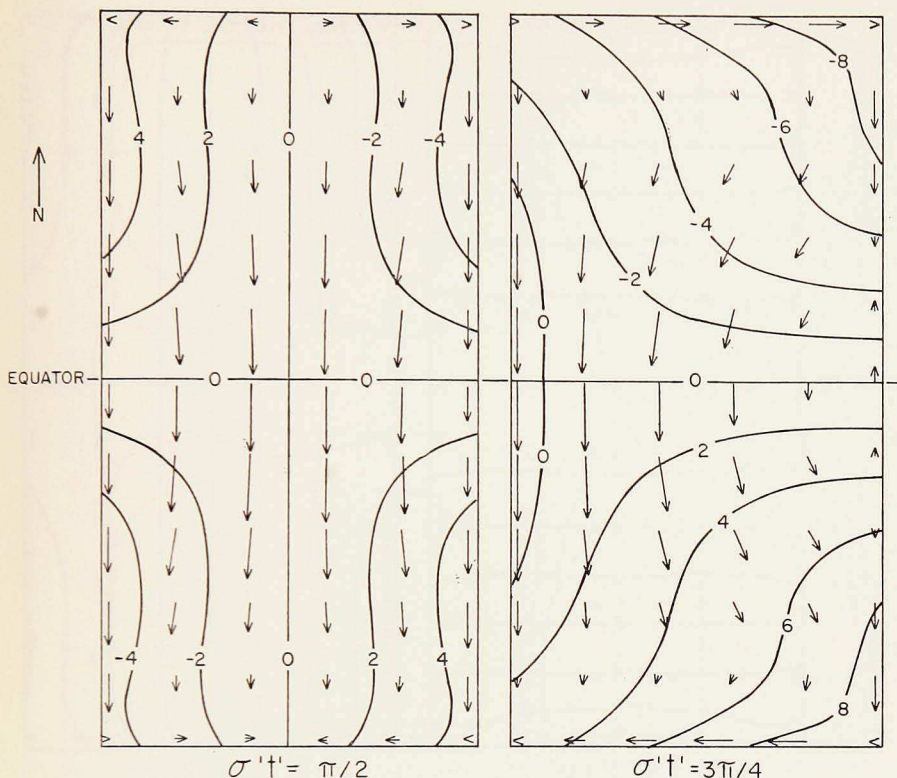


Figure 4 b. Gravity oscillation (0,1), with the lowest frequency for $2x'_0 = y'_0 = 2.12$; period = 1.36 days for $\beta = 2.3(10)^{-13} \text{ cm}^{-1} \text{ sec}^{-1}$, $y_0 = 6.25(10)^3 \text{ km}$. The contours are lines of constant surface elevation, and the arrows are horizontal velocities at the tails of the arrows. See also opposite page.

lation may be interpreted as an equatorial Kelvin wave that propagates along the equator toward the eastern coast, where it splits to form two similar waves that propagate along the coasts to rejoin at the intersection of the equator and the western coast. This is the same description that Moore (1968) gave for the first few modes of internal gravity oscillations; in fact, as the nondimensional size of the ocean increases, the (1,0) and similar oscillations become the gravity oscillations that have the lowest frequencies.

Fig. 6 shows an example of the (1,0) oscillation for an ocean of larger nondimensional size, $2x'_0 = y'_0 = 4.950$. At $\sigma't' = 0$, the equatorial and high-latitude Kelvin waves are clearly discernible; at $\sigma't' = \pi/2$ these waves have propagated around to the meridional coasts. As the waves move along the eastern coast toward a higher latitude, the increasing Coriolis parameter confines the motion more closely to the coasts. Along the western coast, the converse is true, since the waves propagate toward the equator. Since the non-

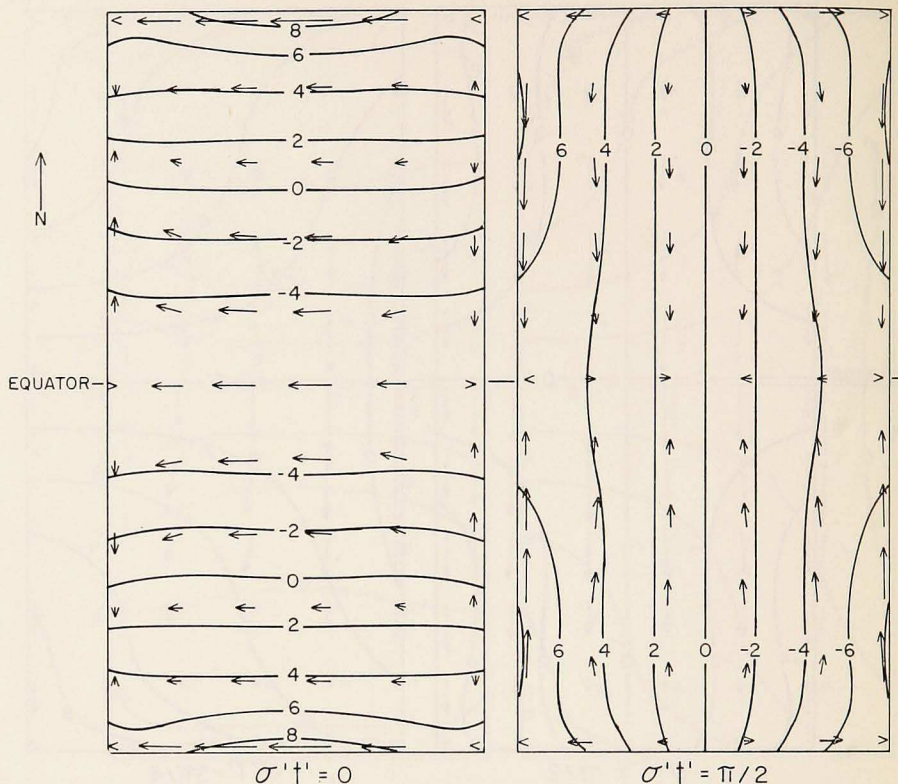


Figure 5. Gravity oscillation (1,0) for $2x'_0 = y'_0 = 2.12$; period = 0.92 days for $\beta = 2.3(10)^{-13}$ $\text{cm}^{-1} \text{sec}^{-1}$, $y_0 = 6.25(10)^3$ km, $H = 4000$ m.

dimensional size of the ocean for the first vertical (internal) mode is roughly $2x'_0 \sim y'_0 \sim 20$, the (1,0) oscillation in this case is much more closely confined to the equator and coasts.

The dynamics governing the gravity oscillation (0,2) for $2x'_0 = y'_0 = 2.12$ are different from those governing the first two. In Fig. 7 we see that the relationship between the velocity and the surface elevation tends toward anti-grotophy, where both the gradient of Z and the Coriolis effect accelerate the water in the same direction. This same relationship occurs in Poincaré waves that propagate in an infinitely long channel with constant f .

Another characteristic of such Poincaré waves is that the frequency must be greater than the Coriolis parameter f . In the (0,2) gravity oscillation, the amplitude of the motion decreases with distance from the equator. Beyond the critical latitude, $y'_c = 1.953$, where f becomes greater than the frequency of oscillation, the motion is small. The behavior of Kelvin waves is unaffected by the relative magnitudes of f and the frequency, so that the (0,1) and (1,0)

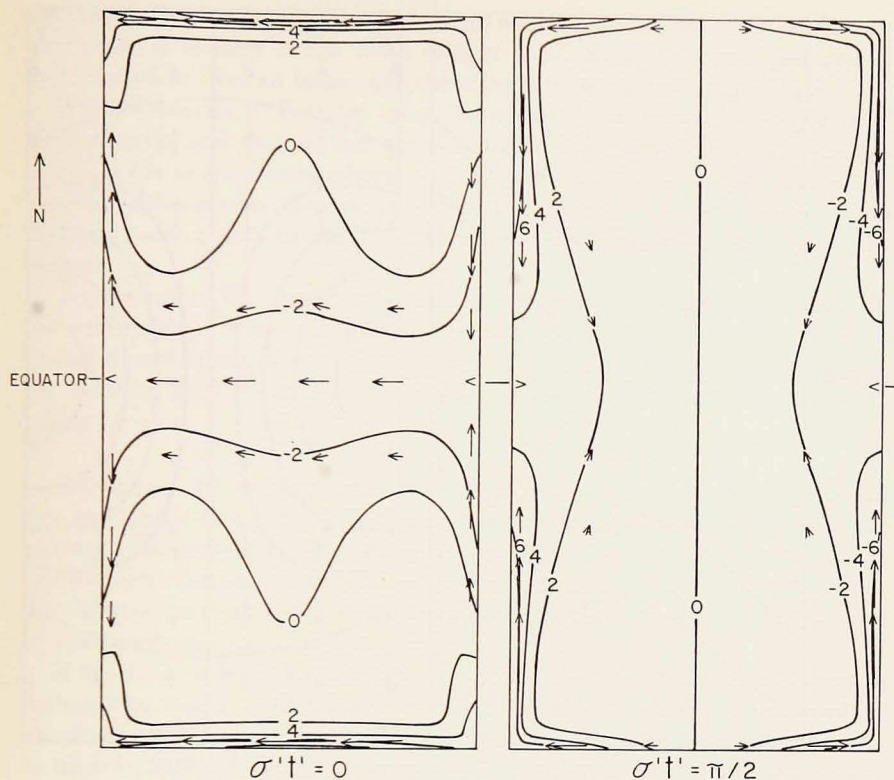


Figure 6. Gravity oscillation (1,0) for a larger ocean, with $2x'_0 = y'_0 = 4.950$.

gravity oscillations, whose dynamics away from the equator resemble those of Kelvin waves, are unaffected by the critical latitude.

For constant f , Corkan and Doodson (1952) found that, as f increases, oscillations like (0,2) become similar in their dynamics to Kelvin waves; Mofjeld (1970) has shown that this occurs also on the beta plane.

ROSSBY OSCILLATIONS. The Rossby oscillation (1,1) is shown in Fig. 8 for a rectangular ocean with $2x'_0 = y'_0 = 2.12$. To present the Rossby oscillations, it is convenient to reduce the scale of the velocities to 0.25 of the scale for the gravity oscillations. At $\sigma^1 t^1 = 0$, the velocity distribution forms a single cell that is centered on the equator, where the maximum velocities occur. Associated with the velocity cell are two cells in the surface elevation that are anti-symmetric about the equator. The motion is nearly geostrophic at high latitude, but it cannot be so around the equator, where the Coriolis parameter is zero. As time increases, cells of opposite sign develop near the eastern coast; at $\sigma^1 t^1 = \pi/2$ there are two sets of cells having equal strength.

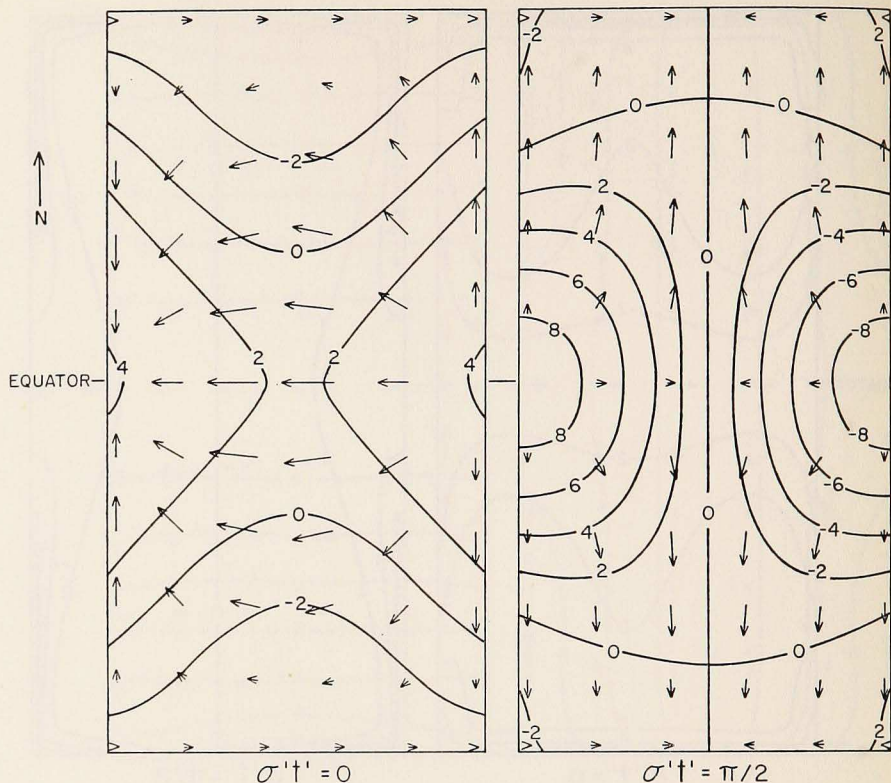


Figure 7. Gravity oscillation (0,2) for $2x'_0 = y'_0 = 2.12$; period = 0.85 days for $\beta = 2.3(10)^{-13}$ $\text{cm}^{-1} \text{sec}^{-1}$, $y_0 = 6.25(10)^3$ km, $H = 4000$ m.

The Rossby oscillation (1,2) in Fig. 9 consists of two cells for both the velocity and surface elevation, Z , at $\sigma't' = 0$ and four cells at $\sigma't' = \pi/2$. While Z is symmetric about the equator, it becomes small in the equatorial region. Higher Rossby oscillations have, in general, larger numbers of cells propagating westward through envelopes that modulate the cells in x and y .

Discussion. By using a bounded beta-plane ocean, we have studied the effects of a free surface, of a variable Coriolis parameter, and of boundaries on one type of time-dependent motion, the free oscillations. To generalize these results to the actual oceans, we must take into account several features of those oceans that are not included in the model. For instance, the actual oceans are not completely bounded but do, in fact, form a connected system.

Rhines (1969), who has demonstrated that Rossby waves can be reflected by abrupt changes in depth, has speculated that higher Rossby oscillations are confined to individual ocean basins by midoceanic ridges. Veronis (1966) has

shown that even a small bottom slope at midlatitude has an effect on Rossby waves that is as large as the effect of beta itself. Variable bottom topography must therefore have an important effect on barotropic motion.

Western-boundary currents may be expected to interact strongly with Rossby waves and may in fact act as sources for Rossby oscillations. Another source is the tropical atmosphere, which, over the Pacific Ocean, has strong 4–5-day fluctuations. Groves and Grivel (1962) have found spectral peaks at 2.7, 4, and 5 days in records taken from tide gauges on islands near the equator.

To determine the dynamic balance that controls time-dependent motion, the relationship between the velocity and the surface elevation must be found; therefore any observational program with this objective must measure the velocity field as well as the surface-elevation field—a difficult undertaking at best.

Conclusions. In this paper we have developed a technique to compute the free oscillations in a rectangular beta-plane ocean placed symmetrically on the equator. The technique may be readily generalized to oceans whose northern and southern boundaries are not at the same distance from the equator. The matrix equation remains unchanged while the eigenfunctions \mathcal{Y}_n and Φ_m must be computed over the new y -interval.

If we think of beta-plane oceans in terms of their nondimensional extent in latitude, the matrix equation approach is applicable to oceans of intermediate extent. If the extent is small, the technique developed by Lamb (1932) may be used for gravity oscillations with small f ; the quasigeostrophic approximation may be used for the Rossby oscillations. When y_0 is sufficiently large, Moore's asymptotic technique is valid, provided that the only motion to reach the northern and southern boundaries is either bound gravity-Rossby waves or Kelvin waves. If, as in the case of internal oscillations (m, n) with a high mode number, n , the free gravity-Rossby waves are affected by these boundaries, then the matrix equation must be used.

The beta-plane ocean has class 1 and class 2 oscillations, which we have called gravity and Rossby oscillations, respectively. For models of the Atlantic and Pacific oceans, the periods of the gravity oscillations are 1.6 days or less and span the periods of the semidiurnal and diurnal tides; the periods of the Rossby oscillations are several days or greater. The periods are, in general, strong functions of the rotation rate, depth, and shape of the ocean.

As Longuet-Higgins and Pond (1970) found for a rotating hemispherical ocean, no two oscillations have the same period. We have seen that, on the beta plane, oscillations also become coupled if their periods are nearly equal, and they cannot have the same period. Oscillations appear to jump from one frequency curve to another if coupling occurs.

The critical latitude, where the Coriolis parameter becomes greater than the

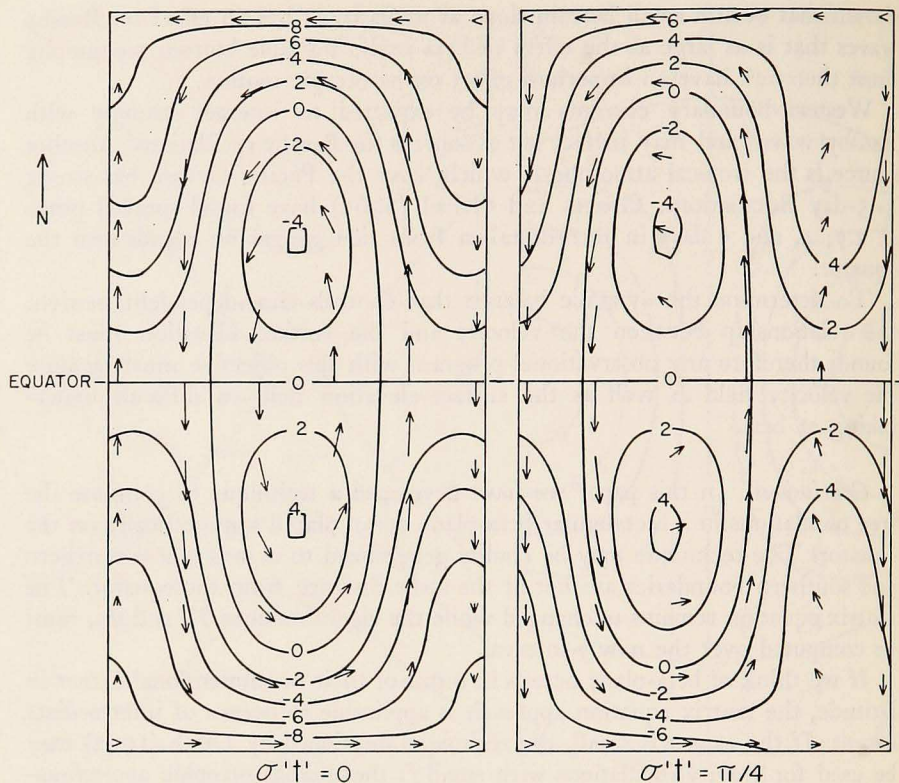


Figure 8a. Rossby oscillations (1,1), with highest frequency for $2x'_0 = y'_0 = 2.12$; period = 3.80 days for $\beta = 2.3(10)^{-13} \text{ cm}^{-1} \text{ sec}^{-1}$ and $y_0 = 6.25(10)^3 \text{ km}$. The velocity scale for the Rossby oscillations has been reduced to 0.25 of the scale for the gravity oscillations. See also opposite page.

frequency, affects only those oscillations for which the Coriolis effect and the gravity accelerate the water in the same direction. These dynamics, typical of Poincaré waves, can exist only if the frequency is greater than the Coriolis parameter.

Rossby oscillations are composed primarily of two gravity-Rossby waves and are therefore similar to the quasigeostrophic oscillations of Rattray and Charnell (1966), except near the resonance with another oscillation. The surface elevation of Rossby oscillations is in general small in the equatorial region compared with the midlatitude. The same is not true of the horizontal velocities.

Acknowledgment. The authors wish to thank F. A. Lee for his advice on numerical techniques and computer programing.

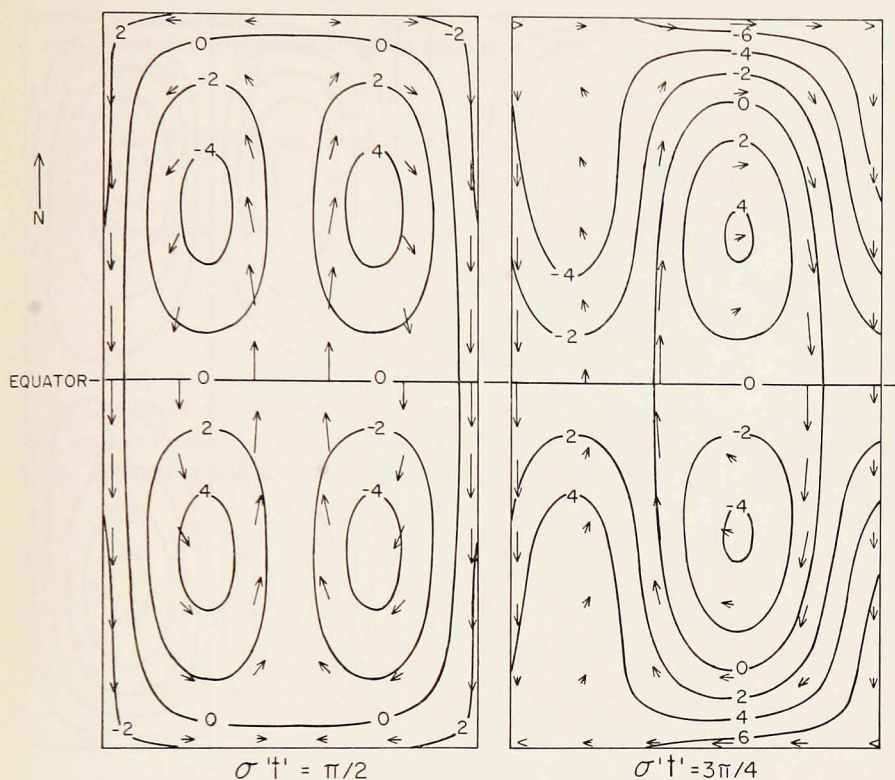


Figure 8b. Rossby oscillation $(1,1)$, with highest frequency for $2x'_0 = y'_0 = 2.12$; period = 3.80 days for $\beta = 2.3(10)^{-13} \text{ cm}^{-1} \text{ sec}^{-1}$ and $y_0 = 6.25(10)^3 \text{ km}$. The velocity scale for the Rossby oscillations has been reduced to 0.25 of the scale for the gravity oscillations. See also opposite page.

REFERENCES

- CORKAN, R. H., and A. Q. DOODSON
1952. Free oscillations in a rotating square sea. *Proc. roy. Soc. London, (A)*215: 147-162.
- FJELDSTAD, J. E.
1933. *Interne Wellen. Geofys. Publ. Kasjoner, 10(6)*: 53 pp.
- GROVES, G. W., and F. P. GRIVEL
1962. Some relationships between sea level and wind in the equatorial Pacific. *Geofys. Intern., Mexico, 2(1)*: 1-14.
- LAMB, HORACE
1932. *Hydrodynamics*, 6th edition. Dover Publications, New York. 738 pp.
- LONGUET-HIGGINS, M. S.
1968. The eigenfunctions of Laplace's tidal equations over a sphere. *Phil. Trans., (A)*262: 511-608.

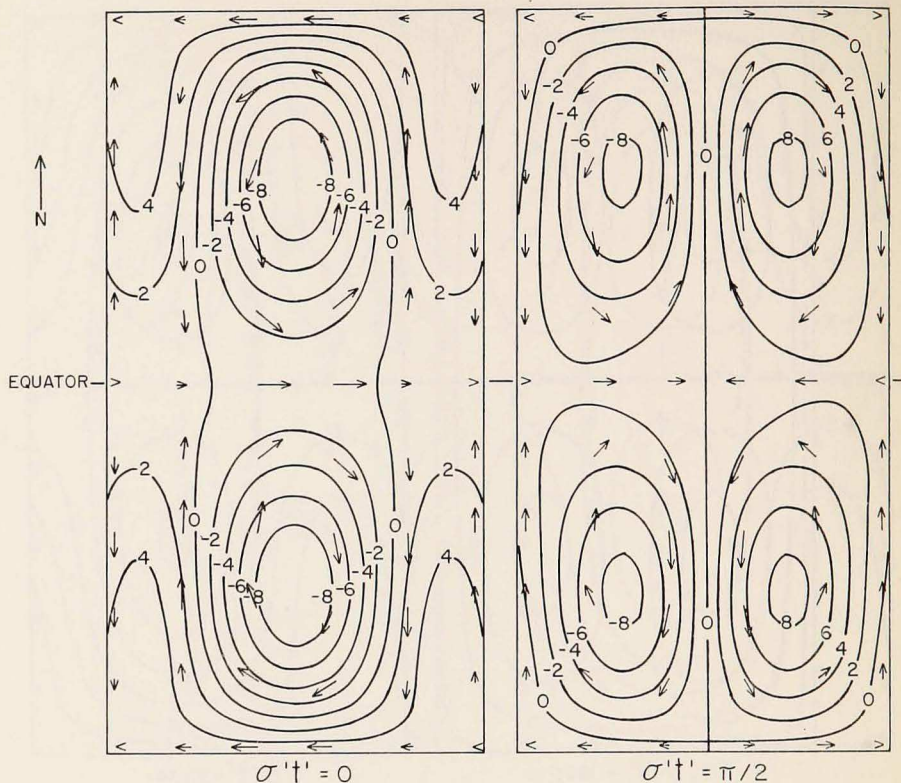


Figure 9. Higher Rossby oscillations (1,2) for $2x'_0 = y'_0 = 2.12$; period = 4.90 days for $\beta = 2.3(10)^{-13}$ $\text{cm}^{-1} \text{sec}^{-1}$ and $y_0 = 6.25(10)^3$ km.

LONGUET-HIGGINS, M. S., and G. S. POND

1970. The free oscillations of fluid on a hemisphere bounded by meridians of longitude. *Phil. Trans., (A)*266: 193-223.

MOFJELD, H. O.

1970. Free oscillations in a bounded, beta-plane ocean. Ph. D. dissertation, University of Washington, Seattle, Washington. 125 pp.

MOORE, DENNIS

1968. Planetary-gravity waves in an equatorial ocean. Ph.D. dissertation, Harvard University, Cambridge, Massachusetts. 207 pp.

RAO, D. B.

1966. Free gravitational oscillations in rotating rectangular basins. *J. fluid Mech.*, 25(3): 523-555.

RATRAY, JR., MAURICE, and R. L. CHARNELL

1966. Quasigeostrophic free oscillations in enclosed basins. *J. mar. Res.*, 24(1): 82-102.

RHINES, P. B.

1969. Slow oscillations in an ocean of varying depth. Part 1. Abrupt topography. *J. fluid Mech.*, 37(1): 161-190.

SCARBOROUGH, J. B.

1966. Numerical mathematical analysis. 6th edition. Johns Hopkins Press, Baltimore, Md. 600 pp.

TAYLOR, G. I.

1922. Tidal oscillations in gulfs and rectangular basins. Proc. London math. Soc., (4)20: 148-181.

VERONIS, GEORGE

1966. Rossby waves with bottom topography. J. mar. Res., 24(3): 338-349.

APPENDIX

In this appendix we give the elements of the matrix U in eq. (42), which was used to compute the frequencies and the amplitudes of the separable solutions. Arranging the amplitude vector as follows

$$\vec{A} = \begin{bmatrix} a_0 \\ b_0 \\ a_1 \\ b_1 \\ - \\ c_n \\ d_n \\ - \end{bmatrix}, \quad (\text{A. 1})$$

the matrix U may be conveniently displayed, using 2 by 2 submatrices

$$U = \begin{bmatrix} U_{1,1} & U_{1,2} & \dots \\ U_{2,1} & U_{2,2} & \dots \\ \dots & \dots & \dots \end{bmatrix}. \quad (\text{A. 2})$$

We then have

$$U_{m,1} = \begin{bmatrix} \cos(\sigma' x'_0) \gamma_{0,m} & \cos(\sigma' x'_0) \delta_{0,m} \\ \sin(\sigma' x'_0) \gamma_{0,m} & -\sin(\sigma' x'_0) \delta_{0,m} \end{bmatrix}; \quad (\text{A. 3})$$

for $R_n^2 = \sigma'^2 + \frac{1}{4\sigma'^2} - \alpha_n > 0$

$$U_{m,n+1} = \begin{bmatrix} \cos \left[\left(\frac{1}{2\sigma'} + R_n \right) x'_0 \right] \gamma_{n,m} & \cos \left[\left(\frac{1}{2\sigma'} - R_n \right) x'_0 \right] \delta_{n,m} \\ \sin \left[\left(\frac{1}{2\sigma'} + R_n \right) x'_0 \right] \gamma_{n,m} & \sin \left[\left(\frac{1}{2\sigma'} - R_n \right) x'_0 \right] \delta_{n,m} \end{bmatrix}; \quad (\text{A. 4})$$

and for $S_n^2 = \alpha_n = \sigma'^2 - \frac{1}{4\sigma'^2} > 0$

$$U_{m, n+1} = \begin{bmatrix} (Q_1 \lambda_{n, m} + Q_2 \mu_{n, m}) & (-Q_1 \mu_{n, m} + Q_2 \lambda_{n, m}) \\ (-Q_3 \lambda_{n, m} + Q_4 \mu_{n, m}) & (-Q_3 \mu_{n, m} - Q_4 \lambda_{n, m}) \end{bmatrix}, \quad (\text{A. 5})$$

where, after absorbing $\cosh(\delta_n x_0)$ into the amplitudes,

$$\left. \begin{aligned} Q_1 &= 2 \cos\left(\frac{x'_0}{2\sigma'}\right), & Q_2 &= 2 \tanh(S_n x'_0) \sin\left(\frac{x'_0}{2\sigma'}\right), \\ Q_3 &= 2 \tanh(S_n x'_0) \cos\left(\frac{x'_0}{2\sigma'}\right), & Q_4 &= 2 \sin\left(\frac{x'_0}{2\sigma'}\right). \end{aligned} \right\} \quad (\text{A. 6})$$

The generalized Fourier coefficients, $\gamma_{0, m}$, $\delta_{0, m}$, etc., correspond to the expansion of γ_0 , δ_0 , etc., in terms of Weber functions, Φ_m , satisfying the differential equation (42) and the zero-slope boundary conditions (43) at $y' = \pm y'_0$. These functions were chosen for the reasonably rapid convergence of the series and for the relatively simple form of the coefficients. Both of the functions Y_n and Φ_m were found by first using a matrix equation to compute the eigenvalues α_n and τ_m and then integrating the differential equations, using Milne's method. These computations are described in detail by Mofjeld (1970), who has also given a derivation of the generalized Fourier coefficients.

For each function ψ that we wish to expand in terms of the set $\{\Phi_m, m = 1, 2, \dots\}$, we have

$$\psi = \sum_{m=1}^{\infty} \langle \psi | \Phi_m \rangle \Phi_m(y), \quad (\text{A. 7})$$

where

$$\langle \psi | \Phi_m \rangle = \int_{-y'_0}^{y'_0} \psi(y') \Phi_m(y') dy'. \quad (\text{A. 8})$$

By making use of the differential equations satisfied by $e^{\pm y'^{2/2}}$ and Φ_m , it is possible to show that

$$\begin{bmatrix} \gamma_{0, m} \\ \delta_{0, m} \end{bmatrix} = \begin{bmatrix} 2A^{(\pm)} y'_0 e^{\pm y'^{2/2}} \Phi_m(y'_0) \\ \tau_m \pm 1 \end{bmatrix}, \quad m \text{ odd}, \quad (\text{A. 9})$$

where the scale factors $A^{(\pm)}$ are added to avoid computational difficulties, and

$$\gamma_{0, m} = \delta_{0, m} = 0, \quad m \text{ even}. \quad (\text{A. 10})$$

Using recursion relations satisfied by $y'Y_n$ and dY_n/dy' , it is also possible to show that

$$\left\langle \frac{dY_n}{dy} \middle| \Phi_m \right\rangle = \begin{cases} -\frac{4y'_0 [dY_n(y'_0)/dy'] \Phi_m(y'_0)}{(\tau_m - \alpha_n)^2 - 4} & (n+m) \text{ odd} \\ 0 & (n+m) \text{ even} \end{cases} \quad (\text{A. 11})$$

and

$$\langle yV_n | \Phi_m \rangle = \begin{cases} \frac{2(\tau_m - \alpha_n)y'_0 [dY_n(y'_0)/dy'] \Phi_m(y'_0)}{(\tau_m - \alpha_n)^2 - 4} & (n+m) \text{ odd} \\ 0 & (n+m) \text{ even} \end{cases} \quad (\text{A. 12})$$

The coefficients $\gamma_{n,m}$, $\delta_{n,m}$, etc., are then, for $n_0 \geq n \geq 1$,

$$\begin{bmatrix} \gamma_{n,m} \\ \delta_{n,m} \end{bmatrix} = \frac{\sigma \langle y'Y_n | \Phi_m \rangle + [(1/2\sigma') \pm R_n] \langle (dY_n/dy') | \Phi_m \rangle}{[\sigma'^2 + (1/4\sigma'^2) + \alpha_n]^{1/2}} \quad (\text{A. 13})$$

and for $n > n_0$

$$\lambda_{n,m} = \frac{\sigma \langle y'Y_n | \Phi_m \rangle + (1/2\sigma') \langle (dY_n/dy') | \Phi_m \rangle}{[\sigma'^2 + (1/4\sigma'^2) + \alpha_n]^{1/2}} \quad (\text{A. 14})$$

and

$$\mu_{n,m} = \frac{S_n \langle (dY_n/dy') | \Phi_m \rangle}{[\sigma'^2 + (1/4\sigma'^2) + \alpha_n]^{1/2}}, \quad (\text{A. 15})$$

where the factor $[\sigma'^2 + (1/4\sigma'^2) + \alpha_n]^{1/2}$ in the denominator has also been added to avoid computational difficulties.